J Polym Res (2013) 20:92
DOI 10.1007/s10965-013-0092-x

ORIGINAL PAPER

# (Re)processing effects on linear low-density polyethylene/silica nanocomposites

**Andrea Dorigato · Alessandro Pegoretti**

Received: 13 November 2012 / Accepted: 20 January 2013


**Abstract** A linear low density polyethylene matrix was melt compounded with a given amount (2 vol.%) of both untreated (hydrophilic) and surface treated (hydrophobic) fumed silica nanoparticles with the aim to investigate the influence of the time under processing conditions on the microstructure and thermo-mechanical properties of the resulting materials. Crosslinking reactions induced by thermal processing caused a remarkable increase of the melt viscosity, as revealed by the melt flow index values of both neat matrix and nanocomposites. Thermal oxidation of the matrix was slightly reduced by the introduction of fumed silica nanoparticles, especially for long compounding times. Differential scanning calorimetry evidenced how silica nanoparticles had a nucleating effect on the matrix, while both the melting temperature and the relative crystallinity were decreased by the compounding process. Nanosilica addition promoted a general improvement of the tensile properties, that progressively decreased with the processing time.

**Keywords** Polyethylene · Silica · Nanocomposites · Thermal stability · Mechanical properties

## Introduction

In the last decades it has been widely proven that the addition of inorganic nanoparticles (such as silica, titania, carbon nanotubes, layered silicates etc.) in polymeric matrices can profoundly modify their properties [1]. Important beneficial effects, such as higher dimensional stability [2], improved moisture and gas barrier properties [3], enhanced mechanical resistance [4–7], and flame retardancy [8] can be obtained even at low filler amounts (< 5 wt.%). The first industrial application of nylon–clay nanocomposites was developed about 20 years ago [9], and since then many efforts were made to develop innovative nanocomposite systems, combining various polymeric matrices and nanofillers [10].

Polyethylene (PE) is one of the most widely used thermoplastic polymers because of its peculiar combination of low cost, high chemical resistance and relatively good mechanical properties. In particular, linear low-density polyethylene (LLDPE) is widely applied in film production for the packaging industry, because of its high tear and impact strength. LLDPE is a copolymer of ethylene and an α-olefin or diene, such as butene, hexene or octene [11]. Therefore, LLDPE is constituted by a linear hydrocarbon backbone with short chain branching. Its relatively poor stiffness and creep resistance, accompanied by a relatively low thermal stability, may limit its application in several fields. The introduction of relatively small amounts of nanoparticles has been proven to play a beneficial role in improving its creep stability [12]. For as the thermal stability and flame resistance are concerned, noticeable improvements were obtained through the introduction of organoclays in PE. The improved flammability resistance induced by layered silicates are generally ascribed to the formation of a clay-enriched protective char during combustion [13, 14]. For instance, Costantino et al. [15, 16] investigated the thermal properties of polyethylene-based nanocomposites containing organically modified hydrotalcites, finding noticeable results in terms of both thermo-oxidative stability and improvements in the combustion behaviour. The morphological behaviour and flammability properties of γ-ray crosslinked maleated polyethylene/clay nanocomposites

A. Dorigato (✉) · A. Pegoretti
Department of Industrial Engineering and INSTM Research Unit, University of Trento, Via Mesiano 77, 38123 Trento, Italy
e-mail: andrea.dorigato@ing.unitn.it

Published online: 03 February 2013

were investigated by Lu et al. [17]. Cone calorimetry tests showed that the increase in heat release rate (HRR) for irradiated materials was suppressed by the nanodispersion of clay layers, especially at elevated irradiation doses.

Quite surprisingly, less attention was devoted in the open literature to polyethylene-based nanocomposite systems filled with isodimensional nanofillers, such as fumed silica nanoparticles. Fumed silica nanoparticles are industrially available in a wide range of specific surface area (ranging from 50 to 400 $m^2 g^{-1}$) and with a variety of surface treatments from hydrophilic to hydrophobic. Due to the elevated specific surface area, this nanofiller is able to self-aggregate when dispersed in polymer matrices, forming an interconnected network of interacting particles [18]. It has been recently demonstrated that the mechanical properties of PE and other thermoplastic matrices can be substantially improved by the introduction of this kind of nanoparticles [4, 12, 18–20].

The thermal stability of polyethylene/silica nanocomposites have also been widely investigated. For instance, Chrissafis et al. [21] studied the thermal degradation mechanism of high density polyethylene (HDPE) containing various amounts of untreated fumed silica nanoparticles. The dispersion of the nanoparticles at the nanoscale produced a remarkable enhancement of the thermal stability, as evidenced by thermogravimetric analysis under non isothermal conditions. Barus et al. [22] synthesized HDPE nanocomposites by dispersing nanosilica particles with and without surface modifiers. Depending on the kind of surfactant employed, thermogravimetric analysis highlighted stabilization phenomena similar to that reported in literature for nanocomposites based on clays, especially in oxidant atmosphere. In a recent wok of our group [23], HDPE based nanocomposites were prepared through a melt compounding process by using various amounts of surface functionalized fumed silica nanoparticles, in order to investigate their capability to improve both mechanical properties and resistance to thermal degradation. The selected nanoparticles resulted to be extremely effective in increasing the decomposition temperature and in decreasing the mass loss rate, even at relatively low filler loadings. Noticeable improvements of the limiting oxygen index (LOI) were detected, especially at elevated silica loadings. Cone calorimeter tests revealed the efficacy of functionalized nanoparticles in delaying the time to ignition (TTI) and in decreasing the heat release rate (HRR) values.

Little is known about the effects of thermal re-processing on the properties of nanofilled thermoplastics [24–29], even if this aspect is surely relevant to establish the possibility to recycle thermoplastic nanocomposites. Thompson and Yeung [24] undertake a multiple-extrusion study on the recyclability of a layered silicate-thermoplastic olefin elastomer nanocomposite. They observed that, despite the occurrence of degradation in the nanocomposite during recycling, its rheological and mechanical properties remained significantly higher than those of the unfilled resin. Chow et al. [25] investigated the effect of a second extrusion on the mechanical behaviour of poly(butylene-terephtalate) composites filled with an organomodified montmorillonite (MMT). It was demonstrated how re-processing on the nanofilled samples marginally affected the original stiffness and the crystallization behaviour of the material. Goitisolo et al. [26] investigated the influence of repeated injection moulding cycles on the mechanical behaviour of polyamide-6/MMT nanocomposites. Even in this case, the introduction of organoclay marginally influenced the dispersion of the filler within the matrix and interfacial adhesion conditions. Also Karahaliou et al. [27] in a study on the thermal re-processing of extruded acrilonitrile-butadiene-styrene/MMT nanocomposites showed how nanofiller introduction played only a marginal role on the rheological and mechanical properties of re-processed samples. Touati et al. [28] investigated the effects of reprocessing cycles on the structure and properties of polypropylene/MMT nanocomposites. They observed that the better dispersion of nanoclay in the nanocomposite induced by repeated extrusion cycles does not necessarily increase the performance of the functional properties such as the thermal and mechanical properties due to the negative effect of polymer degradation. The recyclability of polystyrene/MMT nanocomposites has been investigated by Kaci et al. [29]. They showed that during reprocessing the complementary processes of intercalation improvement and chain scission can balance and yield a stabilization of the mechanical performances of the polystyrene nanocomposites over 8 reprocessing cycles.

To the best of our knowledge, no papers can be found in the open literature on the effects of thermal processing on particulate and/or polyethylene-based nanocomposites. Therefore, in this research project neat LLDPE and nanocomposite samples filled with 2 vol.% of both hydrophilic and hydrophobic fumed silica nanoparticles were prepared through a melt compounding process. The effect of the thermal reprocessing was simulated considering different compounding times and the materials were characterized by rheological tests, scanning electron microscopy, infrared spectroscopy, thermal and mechanical analyses.

## Experimental part

### Materials

A butene copolymer linear low density polyethylene (LLDPE) Flexirene® CL10 was kindly supplied by Polimeri Europa (Mantova, Italy). This LLDPE resin is characterized by a melt

flow index (at 190 °C, 2.16 kg) equal to 2.6 g (10 min)$^{-1}$, a number average molecular weight of 27,000 Da, a density of 0.918 g cm$^{-3}$ and a melting point of 121 °C. Two different kinds of Aerosil® fumed silica were kindly supplied by Degussa (Hanau, Germany). Aerosil® 200 (A200) is an hydrophilic fumed silica, having a density of 2.28 g cm$^{-3}$ and a surface area of 200 m$^2$ g$^{-1}$. Aerosil® R974 (R974) silica nanoparticles are surface treated with dimethyldyclorosilane and have a density of 1.99 g cm$^{-3}$ and a surface area of 170 m$^2$ g$^{-1}$. For both nanoparticles the $SiO_2$ content is higher than 99.8 %. Both LLDPE chips and fumed silica were utilized as received.

### Preparation of the samples

A melt compounding process followed by hot pressing was adopted for sample preparation. A Thermo Haake® internal mixer was used for compounding 2 vol.% of both A200 and R974 silica nanoparticles in LLDPE at 170 °C and 90 rpm. Different compounding times, ranging from 15 min to 360 min (virtually corresponding to 24 cycles of 15 min), were used to simulate the thermal re-processing of the material. The obtained composites were then hot pressed in a Carver® press at 170 °C for 15 min at a pressure of 0.2 kPa, to produce square sheets of 200 200 mm$^2$ with a thickness of about 0.8 mm. The choice of the filler amount was performed with the aim to maximize the tensile strength of the nanocomposites, according to the indications of a previous work on PE/silica nanocomposites [30, 31]. The samples were designated as LLDPE followed by the silica type and the compounding time in minutes. As an example, LLDPE-A200-360 indicates a nanocomposite sample filled with 2 vol.% of Aerosil® 200 fumed silica and processed for a time of 360 min.

### Measurements

Melt flow index (MFI) measurements were performed by a Dynisco 4003DE melt indexer, according to ASTM D1238 standard. Compounded materials were then pelletized and heated at 190 °C, and MFI was measured under an applied weight of 2.16 kg. At least ten measurements were made for each sample.

Field emission scanning electron microscope (FESEM) observations were performed through a Zeiss Supra 40 microscope, operating at an acceleration voltage of 10 kV. Samples were cryofractured in liquid nitrogen and observed at different magnifications after metallization. Fourier transform infrared spectroscopy (FT-IR) tests were conducted by using a Perkin Elmer Spectrum One FT-IR-ATR analyser in a scanning interval between 650 and 4,000 cm$^{-1}$.

Differential scanning calorimetry (DSC) tests were performed by using a Mettler® DSC30 apparatus on specimens having a mass of about 30 mg. A first heating scan from 0 °C to 200 °C was followed by a cooling scan from 200 °C to 0 °C and a second heating scan from 0 °C to 200 °C. All scans were performed at a rate of 10 °C min$^{-1}$ under a nitrogen flow of 100 ml min$^{-1}$. The crystallinity content was evaluated normalizing the melting enthalpy over the standard enthalpy of a fully crystalline polyethylene, taken as 293 J g$^{-1}$ [32].

Quasi-static tensile tests were performed by an Instron® 4502 tensile testing machine equipped with a load cell of 1 kN, on ISO 527 1BA dogbone specimens 5 mm wide and 0.8 mm thick. Elastic modulus was evaluated at a crosshead speed of 0.25 mm min$^{-1}$, and the strain was recorded by an Instron 2620–601 extensometer with a gage length of 12.5 mm. According to ISO 527 standard, the elastic modulus (E) was determined as a secant value between deformation levels of 0.05 % and 0.25 %. Ultimate tensile properties such as stress at break ($\sigma_b$) and strain at break ($\varepsilon_b$) were determined at a crosshead speed of 50 mm min$^{-1}$ without the extensometer. The deformation was estimated by normalizing the crosshead displacement over the gage length of the samples. At least five specimens were tested for each sample.

## Results and discussion

It is well known that the flow behaviour of thermoplastics is strongly affected by the molecular weight and/or by the polydispersity degree and that prolonged thermal treatments could noticeably influence the molecular architecture [33]. Therefore, melt flow index can provide information on the effects of the thermo-mechanical degradative action promoted by melt compounding and the molecular weight of the investigated materials. MFI values of neat LLDPE and of the relative nanocomposites as a function of the processing time are reported in Fig. 1. It can be noticed that MFI values of neat LLDPE strongly decrease with the compounding time, passing from 3.25 g min$^{-1}$ after a compounding interval of 15 min to 0.15 g min$^{-1}$ after a thermal processing of 175 min. According to the literature references [34–39], the observed decrease of the MFI can be associated to crosslinking phenomena due to the thermo-oxidative action of the compounding. It is worthwhile to note that for very long processing times a slight increase of the MFI values can be observed, probably due to chain scission reactions. It is often reported in literature that degradative action of a thermo-oxidative treatment promotes the formation of alchilic radicals (R*) through the rupture of covalent bonds, followed by the reaction with oxygen to form hydroperoxides (ROOH) through a chain reaction, as described in the following scheme :

$$RH \rightarrow R^* \rightarrow RO_2^* \rightarrow ROOH \rightarrow \text{Oxygenated products} \quad (1)$$

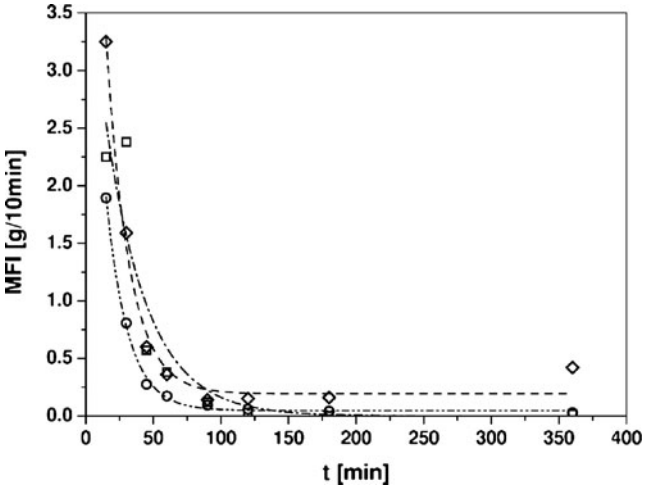


**Fig. 1** Melt flow index (MFI) values as a function of the processing time for neat LLDPE-t (◊), LLDPE-A200-t (□) and LLDPE-R974-t (○) samples ($t$=15–360 min)

The oxygenated reaction products can be alcohols, aldehydes, ketones, acids and esters. Therefore, crosslinking and chain scission reactions are competitive mechanisms in this system, and the decrease of the molecular weight due to thermo-oxidation may prevail only at prolonged thermal exposure.

The addition of hydrophilic fumed silica nanoparticles (A200) determines a noticeable decrease of the MFI values with respect to the unfilled matrix even after a compounding time of 15 min. The increase of the melt viscosity due to nanoparticles introduction is a well known phenomenon [18, 40], and it is generally ascribed to the formation of a percolative network between silica aggregates. MFI values of A200 filled sample are systematically lower than those of the neat LLDPE over the whole range of the investigated compounding times. Interestingly, a prolonged thermal treatment in nanofilled samples does not produce an increase of MFI values. It could be therefore hypothesized that chain scission reactions due to thermal degradation are partially hindered by the presence of silica nanoparticles. Quite similar behaviour can be observed when nanocomposites filled with functionalized nanoparticles (R974) are considered. The stronger decrease of the melt viscosity experienced at low compounding times can be probably attributed to a better dispersion of silica aggregates within the matrix due to the surface modification (as confirmed by FESEM images).

In Fig. 2(a–f) FESEM images of the fracture surfaces of neat LLDPE and of the nanofilled samples with a compounding time of 15 and 360 min are reported. The surface corrugation of fracture surfaces can be attributed to the extremely high ductility of LLDPE [31], and the consequent difficulty to obtain brittle fracture even under cryogenic conditions. The micrographs of LLDPE-A200-15 nanocomposites (Fig. 2c) indicate that fumed silica nanoparticles are uniformly dispersed within the matrix, forming isodimensional clusters of aggregated primary nanoparticles having a mean size of about 200 nm. As reported in our previous papers [18, 23, 40], this aggregated morphology is characteristic of fumed silica, and can be attributed to the strong interaction between the surface hydroxyl groups of the nanoparticles. When a compounding time of 360 min is considered a certain disgregation of the silica aggregates can be observed (Fig. 2d). As expected, a better dispersion with a reduction of the aggregates average dimension can

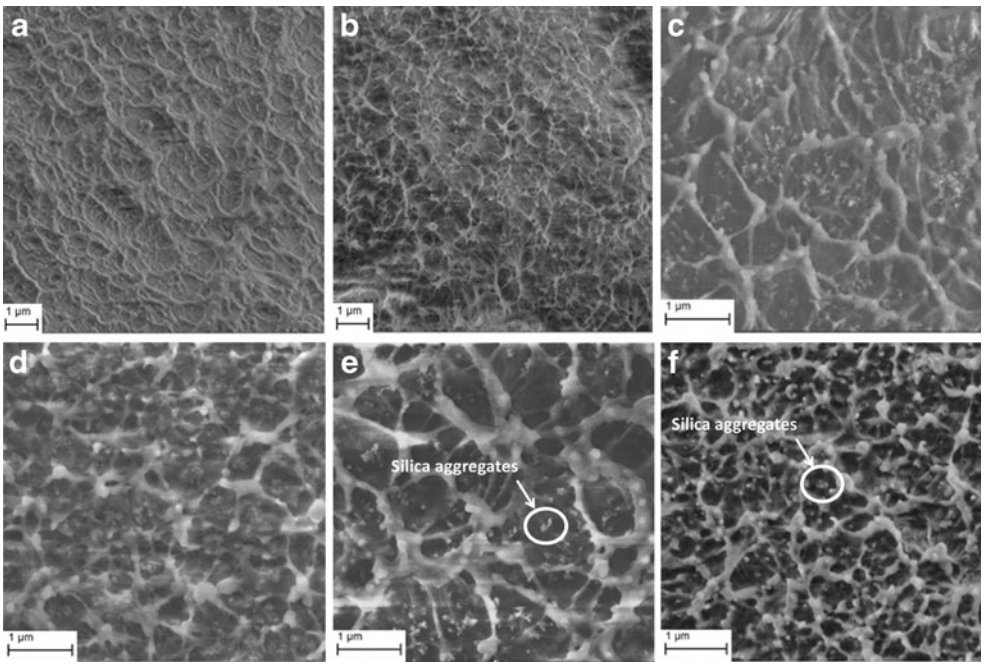


**Fig. 2** FESEM images of the fracture surfaces of **a** LLDPE-15, **b** LLDPE-360, **c** LLDPE-A200-15, **d** LLDPE-A200-360, **e** LLDPE-R974-15 and **f** LLDPE-R974-360 samples

be observed when surface functionalized nanoparticles are used. In fact, on Fig. 2e, f it can be observed that the mean dimension of silica aggregates is reduced to 150 nm, regardless to the compounding duration. Even in this case, a reduction of the silica aggregates can be observed when the processing time increases. It is often reported in the open literature that the surface treatment of inorganic fillers with organic surfactants or coupling agents could lead to a decrease of their surface free energy and thus of their wettability [41]. In these conditions, interparticle interactions are reduced and the nanofiller dispersion within the matrix improved.

As mentioned before, the presence of oxygenated functional groups in the material could be an indication of the thermal oxidation reaction induced by a prolonged thermal processing. FT-IR spectroscopy could be therefore a very sensitive technique to evaluate the effect of the thermo-oxidative degradation process. Fig. 3 reports FT-IR spectra of neat matrix (Fig. 3a) and of the nanofilled samples (Fig. 3b, c) as a function of the compounding time. IR spectra of neat LLDPE samples are characterized by the presence of two characteristic absorbance peaks at 2,920 $cm^{-1}$ and 720 $cm^{-1}$, associated to the asymmetric and symmetric stretching of the C-H bonds, respectively. The absorbance signals at 1,460 $cm^{-1}$ and at 720 $cm^{-1}$ are respectively attributable to the bending and the rocking of $CH_2$ groups [42]. Interestingly, as the compounding time increases a peak located at 1,720 $cm^{-1}$ appears. This peak can be attributed to the stretching of carbonyl groups (C=O). The intensity of this peak rises with the compounding time. According to the literature data, the presence of carbonyls in polyolefins is generally ascribed to thermal oxidation phenomena promoted by prolonged thermal processing [43]. The presence of these functionalities is generally explained considering chain extension reactions under oxygen atmosphere at elevated temperature and the recombination of alchilic radicals [44, 45]. On the FT-IR

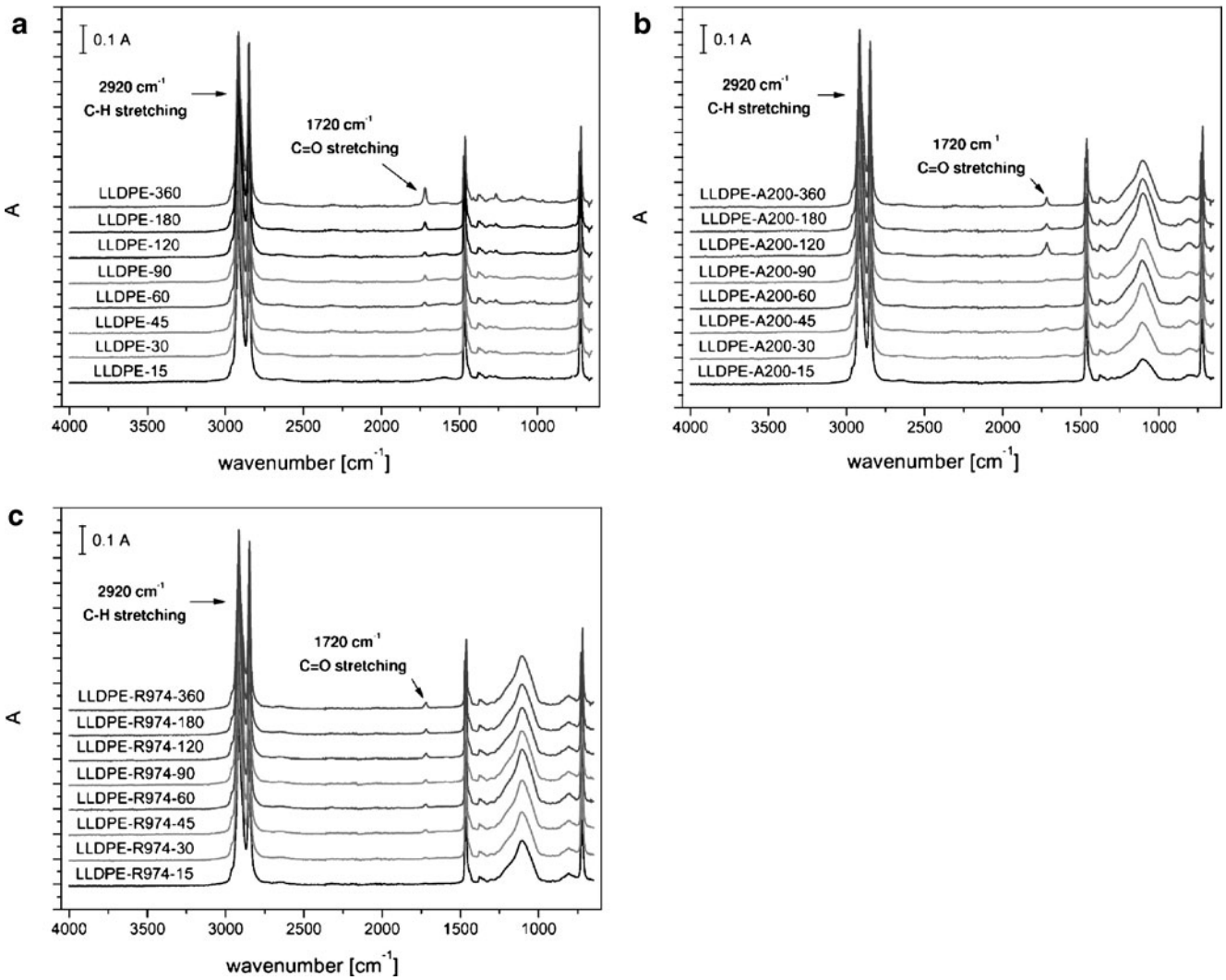


**Fig. 3** FT-IR spectra of **a** LLDPE-t, **b** LLDPE-A200-t and **c** LLDPE-R974-t samples ($t$=15–360 min)

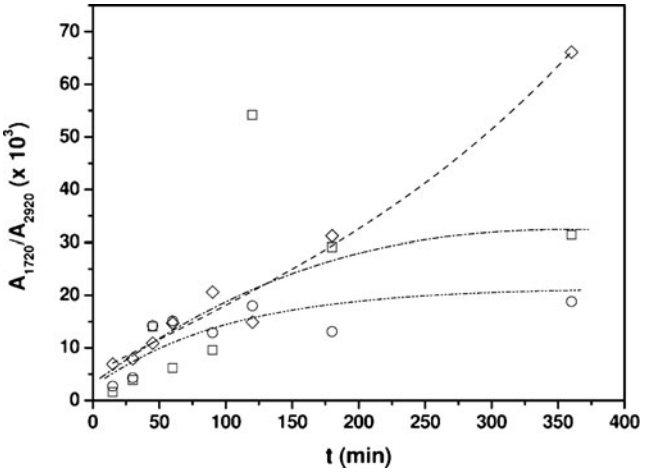


**Fig. 4** Ratio between the absorbance of the carbonylic ($A_{1720}$) and the C-H groups ($A_{2920}$) from FT-IR tests on (◊) LLDPE-t, (□) LLDPE-A200-t and (○) LLDPE-R974-t samples ($t$=15–360 min)

spectra on nanofilled samples (Fig. 3b, c) the presence of two peaks at 1,105 $cm^{-1}$ and 802 $cm^{-1}$, respectively attributable to the asymmetric and symmetric stretching of Si-O-Si groups, can be noticed. Also for nanocomposites the thermal processing promotes chain oxidation, as indicated by the presence of absorbance peaks associated to carbonylic groups (1,720 $cm^{-1}$).

In Fig. 4 the values of the ratio between the absorbance of the carbonylic ($A_{1720}$) and the C-H groups ($A_{2920}$) derived from FT-IR tests on neat LLDPE and on the nanofilled samples at different compounding times are represented. It is evident that the presence of fumed silica in these systems determines a certain reduction of the relative intensity of C=O groups, especially when prolonged compounding times are considered. It is also interesting to note that the presence of the surface functionalization promotes a further reduction of the oxidation phenomena. Therefore, it can be concluded that the presence of fumed silica in these systems hinders the oxidation of the polymer matrix. The higher efficacy of the hydrophobic nanofiller (R974) can be probably attributed to a better dispersion of silica aggregates when a proper surface functionalization is present.

It is well known that thermal degradation could significantly affect thermal properties of polyolefins, and the introduction of inorganic nanofillers can influence both melting and crystallization behaviour. The dependency of the melting temperature ($T_m$) of neat LLDPE and of the relative nanocomposites from the compounding time was evaluated through DSC tests and the results obtained from the first heating scan are reported in Fig. 5a, while in Fig. 5b the crystallinity content ($\chi_C$) is reported. As the compounding time increases the melting point of the crystalline phase of neat LLDPE decreases. This behaviour can be certainly attributed to the fact that thermo-oxidation in polyolefins promotes the presence of crosslinking, lateral ramifications and oxygenated functionalities on the main backbone, that may hinder chain packing and spherulites formation during crystallization, eventually leading to a less ordered crystalline phase [45]. A similar behaviour can be observed also for the investigated nanocomposites. Interestingly, nanofiller introduction determines an increase of the crystallinity degree, regardless to the presence of a surface functionalization. This probably means that, despite their amorphous nature, fumed silica nanoparticles having higher surface area could play some nucleating effect on the LLDPE matrix. This point is still debated in the scientific literature, and some controversial results can be found, especially on polyethylene nanocomposite fibers [46–48]. In our previous works on polyethylene based nanocomposites [12, 18], we have hypothesized that the limited influence played by fumed silica nanoparticles on the crystallization properties of the matrix could be ascribed to their non optimal dispersion state. In

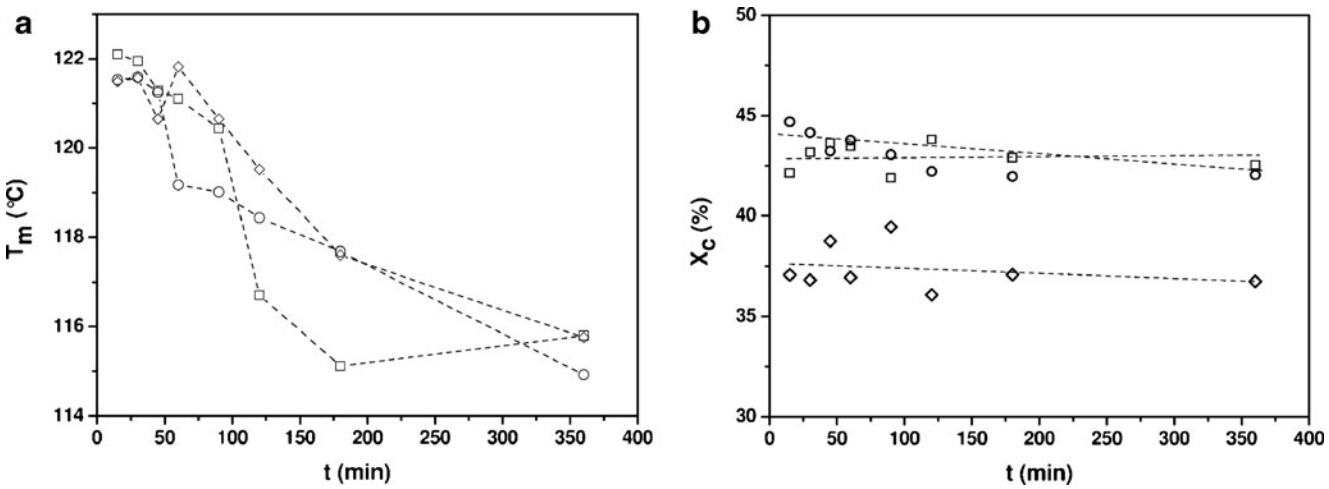


**Fig. 5** Results of DSC first heating scan on (◊) LLDPE-t, (□) LLDPE-A200-t and (○) LLDPE-R974-t samples ($t$=15–360 min). **a** Melting temperature and **b** crystallinity degree

another paper on polyethylene/silica nanocomposites we have found that silica nanoparticles at elevated surface area can promote a slight crystallinity increase [30]. Also the data collected during the cooling scan (reported in Fig. 6) clearly evidence a certain nucleating ability of the silica nanoparticles, which induce a higher crystalline fraction of the nanocomposites with respect to the neat matrix. It is also interesting to observe that the crystallization temperature of the investigated materials markedly decreases with the processing time, as a clear indication that the crystallization process is hindered by the processing-induced crosslinking of the LLDPE matrix.

Representative stress–strain curves of neat LLDPE and of the relative nanocomposites at different processing times, derived from quasi-static tensile tests, are collected in Fig. 7. It is clear that as the processing time increases a remarkable modification of the mechanical response occurs, especially if the ultimate properties are considered. The values of some important tensile properties are plotted in Fig. 8(a–c) at various compounding times for both neat LLDPE and nanocomposites. For as the elastic modulus is concerned, it can be concluded that the stiffness of neat LLDPE is practically unaffected by the compounding time. It can be hypothesized that the stiffening effect induced by the progressive crosslinking at elevated processing times is compensated by the crystallinity drop evidenced by DSC analysis. The introduction of both types of silica nanofiller determines a noticeable increase of the elastic modulus with respect to the neat matrix. For instance, elastic modulus moves from 190 MPa for the neat LLDPE to 286 MPa and 310 MPa for LLDPE-A200-15 and LLDPE-R974-15, respectively. The noticeable increase of the elastic modulus in silica nanofilled samples is well documented in literature, and in a recent paper a new theoretical model was proposed by our group to model the elastic properties of particulate nanocomposites [49, 50]. In that

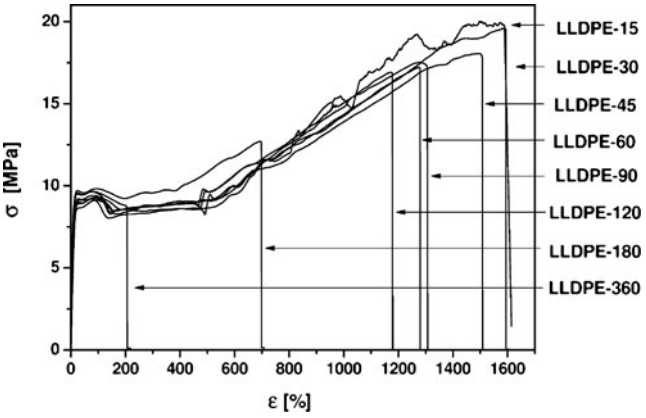


**Fig. 7** Representative stress-stain curves on LLDPE-t samples ($t$=15–360 min)

work it was evidenced how nanofiller aggregation may constrain a portion of matrix, thus limiting the mobility of macromolecules. Interestingly, elastic modulus of nanocomposites decreases with the processing time down to values quite similar to that of the unfilled matrix (see Fig. 8a). This trend could be attributed to a disruption of the silica aggregates provoked by the prolonged compounding time, and the consequent reduction of the stiffening effect related to matrix constrain.

It is also worthwhile to analyze the trends of the ultimate properties with the processing time. On Fig. 8b, c it can be observed that both stress and strain at break of nanocomposites are slightly higher than that of neat matrix. The presence of a surface functionalization on the nanoparticles helps to further improve both $\sigma_b$ and $\varepsilon_b$. These results are in agreement with what previously reported for high density polyethylene-fumed silica nanocomposites [30]. An increase of the processing time leads to a dramatic reduction of the ultimate properties. This strong embrittlement could

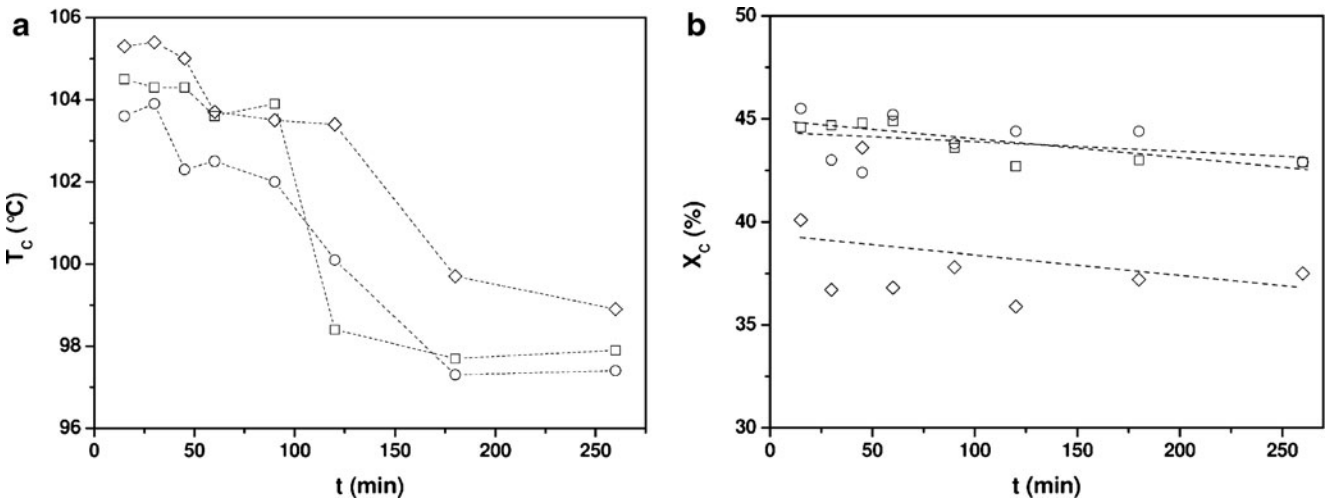


**Fig. 6** Results of DSC cooling scan on (◊) LLDPE-t, (□) LLDPE-A200-t and (○) LLDPE-R974-t samples ($t$=15–360 min). **a** Melting temperature and **b** crystallinity degree

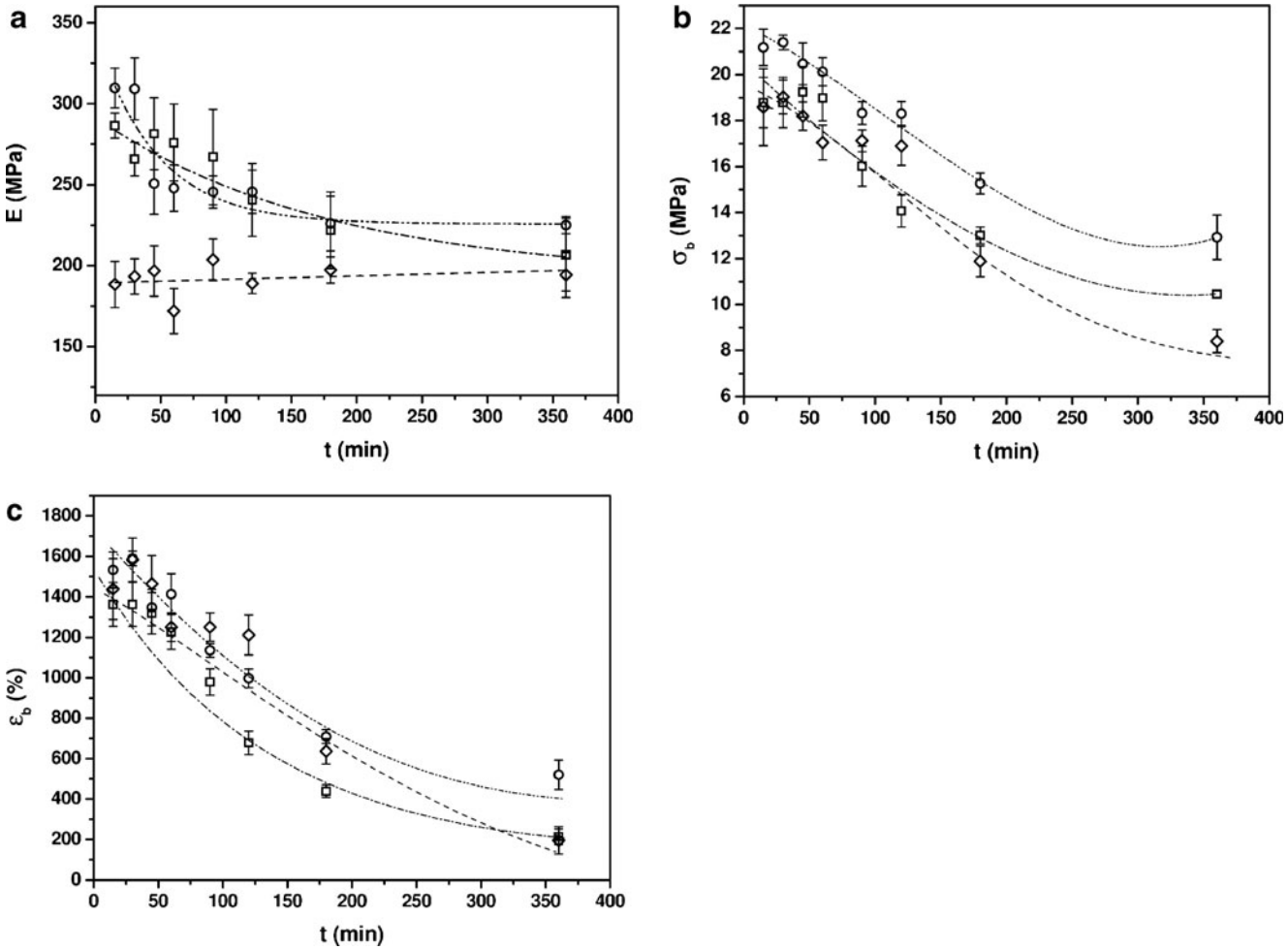


**Fig. 8** **a** Elastic modulus, **b** stress at break and **c** deformation at break of (◊) LLDPE-t, (□) LLDPE-A200-t and (○) LLDPE-R974-t samples ($t$=15–360 min)

be related to the matrix crosslinking occurring under the selected processing conditions. However, the ultimate properties of the nanofilled materials are systematically superior to those of the neat matrix, especially when hydrophobic silica are considered. This beneficial effect could be attributed to the ability of fumed silica nanoparticles to reduce the thermal oxidation of the LLDPE matrix, as evidenced by FTIR analysis.

## Conclusions

Both untreated and surface treated fumed silica nanoparticles were melt compounded in a LLDPE matrix, in order to investigate the influence of the processing duration on the thermo-mechanical behaviour of the resulting materials. MFI measurements evidenced how the viscosity of both neat LLDPE and the nanofilled samples progressively increase with the processing time, due to the crosslinking reactions induced by the thermal processing. FTIR analysis evidenced that fumed silica nanoparticles partially prevented the oxidation of the polymer matrix, especially when long processing times are considered. DSC tests revealed that fumed silica nanoparticles play a nucleating effect on the matrix crystallization, while both the melting and crystallization temperatures and the relative crystallinity were progressively decreased as the processing time increases. Quasi static tensile properties were improved by nanofiller addition, while both the stress and the strain at break progressively decreased with the processing time.

**Acknowledgments** Mr. Umberto Saccoman is gratefully acknowledged for his valuable support to the experimental work.

## References

1. Bondioli F, Dorigato A, Fabbri P, Messori M, Pegoretti A (2008) High-density polyethylene reinforced with submicron titania particles. Polym Eng Sci 48:448–457

2. Bondioli F, Dorigato A, Fabbri P, Messori M, Pegoretti A (2009) Improving the creep stability of high-density polyethylene with acicular titania nanoparticles. J Appl Polym Sci 112:1045–1055
3. Kim JK, Hu C, Woo RSC, Sham ML (2005) Moisture barrier characteristics of organoclay–epoxy nanocomposites. Compos Sci Technol 65:805–813
4. Kontou E, Niaounakis M (2006) Thermo-mechanical properties of lldpe/sio2 nanocomposites. Polymer 47:1267–1280
5. Pegoretti A, Dorigato A, Penati A (2007) Tensile mechanical response of polyethylene – clay nanocomposites. Expr Pol Lett 1 (3):123–131
6. Pegoretti A, Dorigato A, Penati A (2008) Contact angle measurements as a tool to investigate the filer-matrix interactions in polyurethane-clay nanocomposites from blocked prepolymer. Eur Polym J 44:1662–1672
7. Dimitry OIH, Abdeen ZI, Ismail EA, Saad ALG (2010) Preparation and properties of elastomeric polyurethane/organically modified montmorillonite nanocomposites. J Polym Res 17:801–813
8. Zhang J, Jiang DD, Wilkie CA (2005) Fire properties of styrenic polymer–clay nanocomposites based on oligomerically-modified clay. Polym Degrad Stab 91:358–366
9. Kojima Y, Usuki A, Kawasumi M, Kojima Y, Fukushima Y, Okada A (1993) Mechanical properties of nylon 6 – clay hybrid. J Mater Res 8:1185–1189
10. Supova M, Martynkova GS, Barabaszova K (2011) Effect of nanofillers dispersion in polymer matrices: a review. Sci Adv Mater 3:1–25
11. Malpass DB (2010) Introduction to industrial polyethylene. Co-published by John Wiley & Sons and Scrivener Publishing LCC, Salem
12. Dorigato A, Pegoretti A, Kolarik J (2010) Nonlinear tensile creep of linear low density polyethylene/fumed silica nanocomposites: time-strain superposition and creep prediction. Polym Compos 31:1947–1955
13. Gilman JW (1999) Flammability and thermal stability studies of polymer layered-silicate (clay) nanocomposites. Appl Clay Sci 15 (1–2):31–49
14. Kiliaris P, Papaspyrides CD (2010) Polymer/layered silicate (clay) nanocomposites: an overview of flame retardancy. Prog Polym Sci 35:902–958
15. Costantino U, Gallipoli A, Nocchetti M, Camino G, Bellucci F, Frache A (2005) New nano-composites constituted of polyethylene and organically modified znal-hydrotalcites. Polym Degrad Stab 90:586–590
16. Costantino U, Montanari F, Nocchetti M, Canepa F, Frache A (2007) Preparation and characterization of hydrotalcite/carboxy-adamantane intercalation compounds as fillers of polymeric nanocomposites. J Mater Chem 17:1079–1086
17. Lu H, Hu Y, Xiao J, Kong Q, Chen Z, Fan W (2005) The influence of irradiation on morphology evolution and flammability properties of maleated polyethylene/clay nanocomposite. Mater Lett 59:648–651
18. Dorigato A, Pegoretti A, Penati A (2010) Linear low-density polyethylene/silica micro- and nanocomposites: dynamic rheological measurements and modelling. Expr Pol Lett 4(2):115–129
19. Dorigato A, Fambri L, Pegoretti A, Slouf M, Kolarik J (2011) Cycloolefin copolymer (coc)/fumed silica nanocomposites. J Appl Polym Sci 119:3393–3402
20. Dorigato A, Pegoretti A (2010) Tensile creep behaviour of polymethylpentene/silica nanocomposites. Polym Int 59:719–724
21. Chrissafis K, Paraskevopoulos KM, Pavlidou E, Bikiaris D (2009) Thermal degradation mechanism of hdpe nanocomposites containing fumed silica nanoparticles. Thermochim Acta 485:65–71
22. Barus S, Zanetti M, Lazzari M, Costa L (2009) Preparation of polymeric hybrid nanocomposites based on pe and nanosilica. Polymer 50:2595–2600
23. Dorigato A, Pegoretti A, Frache A (2012) Thermal stability of high density polyethylene–fumed silica nanocomposites. J Therm Anal Calorim 109:863–873
24. Thompson MR, Yeung KK (2006) Recyclability of a layered silicate-thermoplastic olefin elastomer nanocomposite. Polym Degrad Stab 91(10):2396–2407
25. Chow WS (2008) Cyclic extrusion of poly(butylene terephthalate)/organo-montmorillonite nanocomposites: thermal and mechanical retention properties. J Appl Polym Sci 110:1642–1648
26. Goitisolo I, Equiazabal JI, Nazabal J (2008) Effects of reprocessing on the structure and properties of polyamide 6 nanocomposites. Polym Degrad Stab 93:1747–1752
27. Karahaliou EK, Tarantili PA (2009) Preparation of poly(acrylonitrile–butadiene–styrene)/montmorillonite nanocomposites and degradation studies during extrusion reprocessing. J Appl Polym Sci 113:2271–2281
28. Touati N, Kaci M, Bruzaud S, Grohens Y (2011) The effects of reprocessing cycles on the structure and properties of isotactic polypropylene/cloisite 15a nanocomposites. Polym Degrad Stab 96(6):1064–1073
29. Kaci M, Remili C, Benhamida A, Bruzaud S, Grohens Y (2012) Recyclability of polystyrene/clay nanocomposites. Mol Cryst Liq Cryst 556:94–106
30. Dorigato A, D'Amato M, Pegoretti A (2012) Thermo-mechanical properties of high density polyethylene—fumed silica nanocomposites: effect of filler surface area and treatment. J Polym Res 19:9889–9899
31. Dorigato A, Pegoretti A (2012) Fracture behaviour of linear low density polyethylene – fumed silica composites. Eng Fract Mech 79(1):213–224
32. Mark HF (2004) Encyclopedia of polymer science and technology, 3rd edn. Wiley, New York
33. Gupta RK (2000) Polymer and composite rheology. Dekker, New York
34. Barabas K, Iring M, Kelen T (1976) Study of the thermal oxidation of polyolefins. V. Volatile products in the thermal oxidation of polyethylene. J Polym Sci 57:65–71
35. Bikiaris D, Prinos J, Panayiotou C (1997) Effect of eaa and starch on the thermooxidative degradation of ldpe. Polym Degrad Stab 56:1–9
36. Bikiaris D, Prinos J, Perrier C, Panayiotou C (1997) Thermoanalytical study of the effect of eaa and starch on the thermo-oxidative degradation of ldpe. Polym Degrad Stab 57:313–324
37. Eriksson E, Johansson E, Kettaneh-Wold N (2001) Multi- and megavariate data analysis principles and applications. Umetrics Academy, New York
38. Holmstrom A, Sorvik E (1970) Thermal degradation of polyethylene in a nitrogen atmosphere of low oxygen content: I. Changes in molecular weight distribution. J Chromatogr 53:95–108
39. Gugumus F (2000) Physico-chemical aspects of polyethylene processing in an open mixer6. Discussion of hydroperoxide formation and decomposition. Polym Degrad Stab 68:337–352
40. Ajayan PM, Schadler LS (2003) Nanocomposite science and technology. Wiley-VCH, Weinheim
41. Naveau E, Dominkovics Z, Detrembleur C, Jerome C, Harim J, Renner K, Alexandre M, Pukanszky B (2011) Effect of clay modification on the structure and mechanical properties of polyamide-6 nanocomposites. Eur Polym J 47(1):5–15
42. Silverstein RM, Bussler GC, Morril TC (1981) Spectroscopic identification of of organic compounds. Wiley, New York
43. Jing X, Chen E, Me E (1992) Applied directory of infrared-photoacustic spectroscopy. Tjanjin Science and Technology Press, Tjanjin
44. Holmstrom A, Sorvik E (1974) Thermal degradation of polyethylene in a nitrogen atmosphere of low oxygen content. Iii. Structural changes occurring in low-density polyethylene at oxygen contents below 1.2 %. J Appl Polym Sci 18:3153–3158

45. Holmstrom A, Sorvik EM (1978) Thermooxidative degradation of polyethylene. I and ii. Structural changes occurring in low-density polyethylene, high-density polyethylene, and tetratetracontane heated in air. J Polym Sci Part A: Polym Chem 16:2555–2586
46. La Mantia FP, Dintcheva NT, Scaffaro R, Marino R (2008) Morphology and properties of polyethylene/clay nanocomposite drawn fibers. Macromol Mater Eng 293:83–91
47. Ruan S, Gao P, Yu TX (2006) Ultra-strong gel-spun uhmwpe fibers reinforced using multiwalled carbon nanotubes. Polymer 47:1604–1611
48. Zhang Y, Yu J, Zhou C, Chen L, Hu Z (2010) Preparation, morphology, and adhesive and mechanical properties of ultrahigh-molecular-weight polyethylene/sio2 nanocomposite fibers. Polym Compos 31:684–690
49. Dorigato A, Dzenis Y, Pegoretti A (2012) On the reinforcement mechanism in particulate nanocomposites. Mech Mater (in press)
50. Dorigato A, Dzenis Y, Pegoretti A (2011) Nanofiller aggregation as reinforcing mechanism in nanocomposites. Procedia Eng 10:894–899